Nature Communications

https://doi.org/10.1038/s41467-026-69591-x

Article in Press

A synergistic design model for ultrathin broadband microwave absorbers using electromagnetic frequency dispersion coefficients

Received: 29 October 2025

Accepted: 29 January 2026

Cite this article as: Si, H., Zhang, Y., Li, M. *et al.* A synergistic design model for ultrathin broadband microwave absorbers using electromagnetic frequency dispersion coefficients. *Nat Commun* (2026). https://doi.org/10.1038/s41467-026-69591-x

Haoxu Si, Yi Zhang, Mu Li, Zehui Chai, Jingwei Zhang, Cuiping Li & Chunhong Gong

A Synergistic Design Model for Ultrathin Broadband Microwave Absorbers Using Electromagnetic Frequency Dispersion Coefficients

Haoxu Si[1, 2#], Yi Zhang[1#], Mu Li[1], Zehui Chai[1], Jingwei Zhang[2*], Cuiping Li[2], Chunhong Gong[1*]

[1] Institute of Functional Polymer Composites, College of Chemistry and Molecular Sciences, Henan University, Kaifeng 475004, China

[2] National & Local Joint Engineering Research Center for Applied Technology of Hybrid Nanomaterials, Henan University, Kaifeng 475004, China

[*] Corresponding authors.

E-mail addresses: jwzhang@henu.edu.cn (J. Zhang); gong@henu.edu.cn (C. Gong).

[#]These authors contributed equally to this work.

Abstract

Ultrathin, broadband microwave absorbing materials (MAMs) are crucial for weight-sensitive and space-constrained applications. This study introduces the electromagnetic frequency dispersion coefficient (EFDC), a synergistic dielectric-magnetic parameter that moves beyond conventional complex mechanisms. Our model directly links EFDC to microwave absorption (MA) performance, guiding the design of advanced MAMs. By optimizing EFDC, we achieved an ultra-wide effective absorption bandwidth (EAB) of 7.04 GHz at 1 mm and 9.28 GHz at 1.3 mm. Moreover, the temperature invariance of EFDC ensures consistent MA performance from 298 K to 473 K, despite the differing thermal responses of permittivity and permeability. This principle outlines a systematic design strategy for fabricating ultrathin and broadband MAMs, establishing a robust framework for developing high-attenuation absorbers suitable for complex frequency and thermal environments.

Introduction

With the rapid advancement of electronic information technology, the widespread application of electromagnetic waves (EMWs) has underscored the urgent need to address electromagnetic interference and compatibility issues in electronic devices[1-4]. This growing concern has stimulated increasing demand for high-performance microwave absorbing materials (MAMs)[5-8]. Driven by the ongoing integration and miniaturization of electronic communication devices and chips, ultrathin MAMs offer substantial advantages in terms of weight reduction and spatial efficiency, making them highly desirable for integrated industries such as aerospace[9], automotive engineering[10], mobile telecommunications[11], and portable electronics[12]. These applications impose stringent requirements on MAMs, including minimal thickness, broad effective absorption bandwidth (EAB, defined as RL < -10 dB), and strong absorption intensity[13,14], all of which are essential for ensuring optimal performance under complex frequency and temperature conditions. According to transmission line theory, the propagation of EMWs in a medium is strongly influenced by the complex permittivity ($\varepsilon_r = \varepsilon_r' - j\varepsilon_r''$) and complex permeability ($\mu_r = \mu_r' - j\mu_r''$) of MAMs[15-17]. These parameters play a critical role in determining both the operating frequency and the overall absorption efficiency, making their optimization central to absorber design. Although significant progress has been made in developing dielectric-magnetic hybrid absorbers through experimental studies, the underlying physical mechanisms governing performance optimization remain inadequately elucidated[18-20]. The Planck-Rozanov limit, expressed as $\Delta\lambda/d < (16\mu_r)/(ln\rho_0)$, where $\Delta\lambda$ denotes the wavelength variation across the operating band, d is the absorber thickness, and ρ_0 is the reflection coefficient, highlights a

fundamental constraint in simultaneously achieving broad bandwidth and reduced thickness[21]. For instance, when the absorption intensity exceeds 90%, the corresponding $\Delta\lambda/d$ value is typically below 13.9, suggesting that thinner MAMs often suffer from insufficient EAB. While the introduction of multiple loss mechanisms and innovative structural designs has been shown to enhance absorption intensity and bandwidth, a reduction in thickness—particularly below 2 mm—frequently leads to compromised attenuation capability[22-25]. Consequently, achieving high absorption performance and broad EAB in ultrathin MAMs remains a considerable challenge, necessitating precise control over the frequency dispersion of electromagnetic parameters[26].

Conventional design of microwave absorbers has largely relied on extensive experimental iterations to empirically adjust ε_r and μ_r, due to the complex interplay and coupling between these parameters. From the wave nature of EMWs, it is known that interference cancellation can substantially enhance microwave absorption performance in a manner unparalleled by other loss mechanisms, and over a wide frequency range. The effective wavelength within the medium, $\lambda_m = c/(f|\mu_r\varepsilon_r|^{1/2})$, depends on both the operating frequency and the electromagnetic parameters of the medium[27]. For each frequency, there exists an optimal $|\mu_r\varepsilon_r|$ value that maximizes absorption. Thus, comprehending the correlation between $|\mu_r\varepsilon_r|$ and frequency is crucial for evaluating its influence on absorption efficiency and the corresponding absorption frequency. Rather than examining permittivity and permeability in isolation, this study introduces the Electromagnetic Frequency Dispersion Coefficient ($EFDC = |\mu_r\varepsilon_r|$) as a unified dielectric-magnetic parameter for optimizing microwave absorption. The model linking EFDC to absorption performance provides a direct framework for tailoring MA characteristics by simultaneously

accounting for the contributions of both complex permittivity and permeability, thereby facilitating either targeted band or broadband absorption design.

In this work, a magnetic-dielectric composite was developed for ultrathin broadband MAMs, comprising carbonyl iron powder (CIP) as the magnetic component and carbon nanotubes (CNTs) as the dielectric phase. Using a feedforward neural network (FNN) model, optimal EFDC values were predicted across various frequencies and thicknesses. The refined relationship between EFDC and frequency significantly aids in the rational design of advanced MAMs. As a result, a CIP/CNTs/EP composite with a thickness of only 1 mm achieves an exceptional EAB of 7.04 GHz. The specific EAB efficiency (SEAB), defined as EAB per unit thickness (EAB d^{-1}), serves as a key figure of merit for applications demanding thin and wideband absorption. The remarkable SEAB value of 7.04 GHz mm^{-1} demonstrated here exceeds those reported in many previous studies[28-30]. Furthermore, although both ε_r and μ_r exhibit opposing trends in their temperature dependence (298 K to 473 K), the collective contribution to absorption performance remains stable due to the consistent behavior of EFDC. This study also proposes a systematic strategy for decoupling microwave absorption behavior from temperature effects—shifting the focus from the pursuit of temperature-invariant electromagnetic parameters to an optimized model that correlates synergistic EM contributions with absorption metrics. The conceptual framework of the electromagnetic synergy strategy based on EFDC is depicted in Fig. 1. This framework not only facilitates the development of ultrathin, broadband MAMs, but also provides innovative insights for the targeted design of high-performance absorbers capable of operating across diverse frequency ranges and under varying thermal conditions.

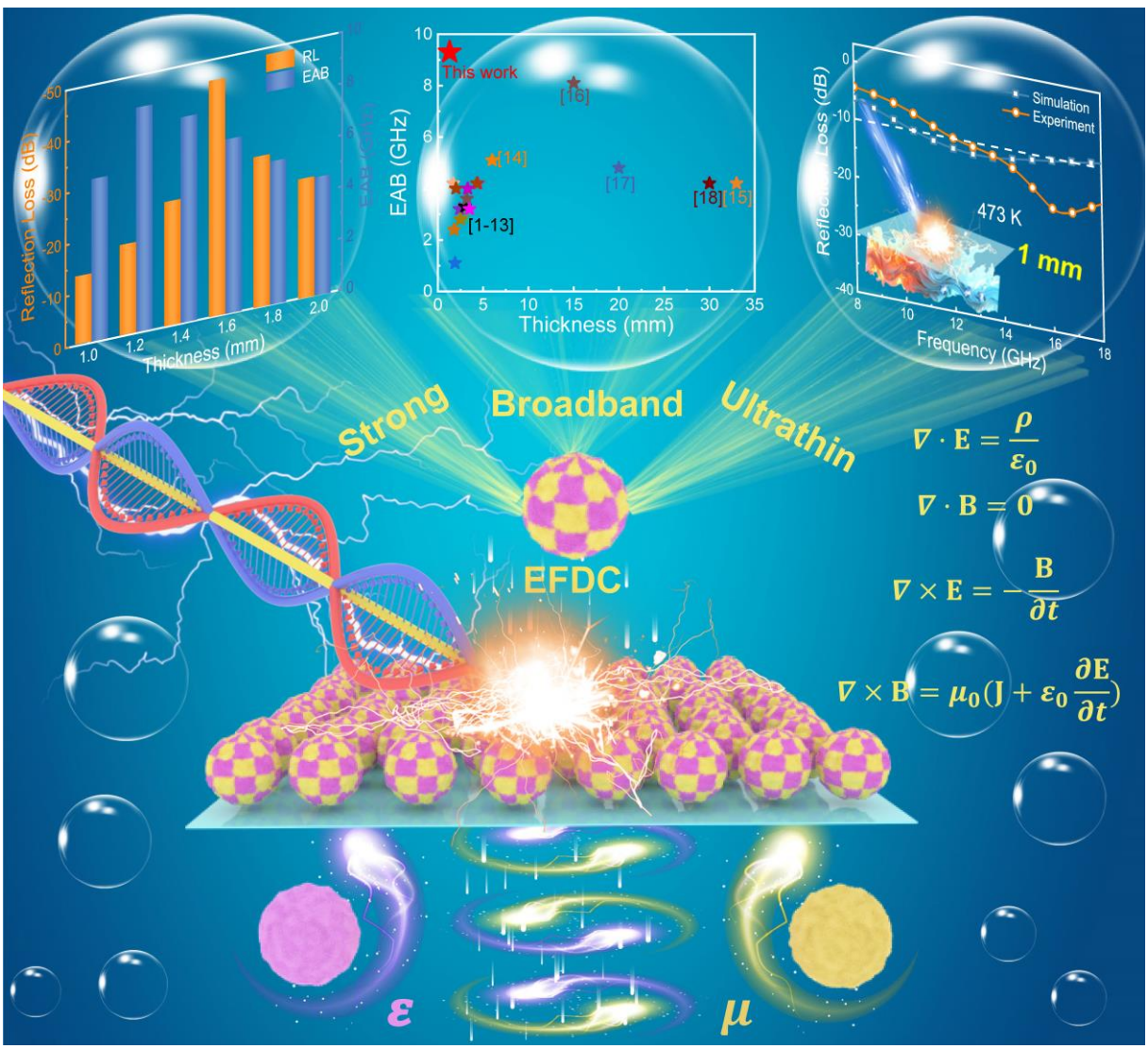

Fig. 1 | Conceptual illustration of the electromagnetic synergy strategy based on electromagnetic frequency dispersion coefficient (EFDC). In this framework, the concurrent interactions between the electric and magnetic fields of electromagnetic waves and the medium result in improved absorption performance.

Results

Establishment of electromagnetic frequency dispersion coefficient models

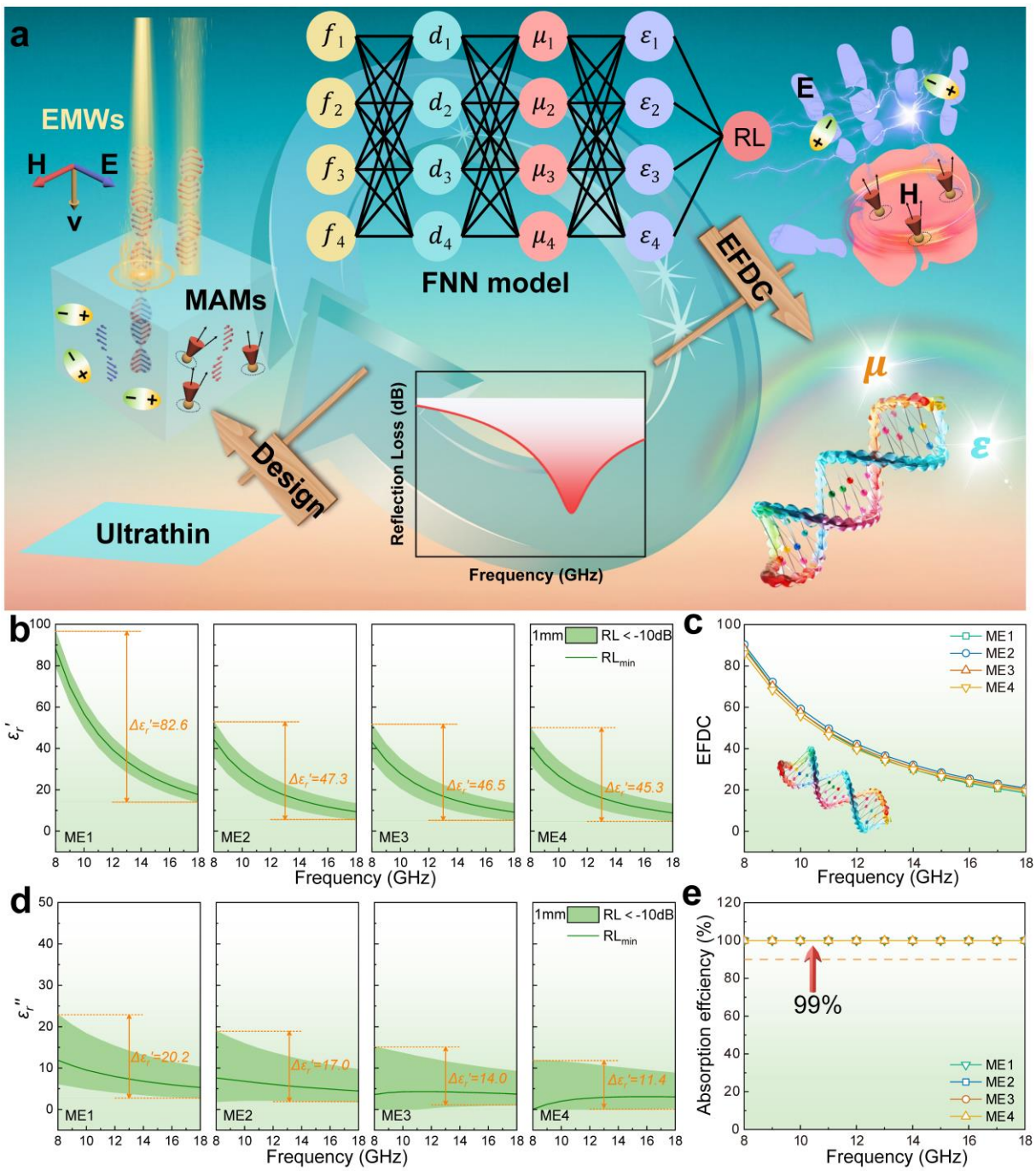

Fig. 2 | Proposal and establishment of electromagnetic frequency dispersion coefficient (EFDC) based on the concept of electromagnetic synergistic. a Design strategy for ultrathin broadband MAMs. Frequency-dependent **b** real permittivity (ε_r'), **c** electromagnetic frequency dispersion coefficient, **d** imaginary permittivity (ε_r''), and **e** microwave absorption performance for

model systems ME1–ME4 at a thickness of 1 mm. The complex permeability values (μ_r' and μ_r'') for ME1, ME2, ME3, and ME4 are (1, 0), (2, 0.2), (2, 0.4), and (2, 0.6), respectively. The shaded region indicates the optimal range of ε_r for effective microwave absorption performance (RL $<$ −10 dB).

According to transmission line theory, achieving efficient MA performance across a broad frequency spectrum necessitates the coordinated optimization of both electromagnetic parameters and their frequency dispersion characteristics. To realize effective MA performance (RL $<$ −10 dB), the optimal frequency-dependent permittivity (ε_r-f) distributions for various thicknesses (1 mm, 2 mm, and 3 mm) were determined using a feedforward neural network (FNN) model. For a typically dielectric system, the relative permeability was fixed at μ_r' = 1 and μ_r'' = 0. As shown in Supplementary Fig. 1, thinner MAMs exhibit more pronounced variations in in both the real (ε_r') and imaginary (ε_r'') parts of permittivity. Specifically, at a thickness of 1 mm, the ε_r-f curve displays a steep descending profile. The material properties required for low-frequency absorption differ considerably from those suited to high-frequency applications, indicating that distinct relaxation strengths and dispersion behaviors are essential across different bands. Notably, the required relaxation strength ($\Delta\varepsilon_r'$) in the range of 8–18 GHz can reach values as high as 82.6. Such a sharp decline in ε_r, coupled with high relaxation strength, poses a significant challenge for achieving these properties in naturally occurring or single-phase materials.

The attenuation of EMWs stems from the synergistic interaction between electric and magnetic fields. Introducing magnetic loss into dielectric composites enhances MA performance through

two primary mechanisms: first, by augmenting the overall attenuation capacity via multi-loss synergy; and second, by improving impedance matching through optimized electromagnetic coupling[31-36]. Consequently, the demanding dispersion behavior that is difficult to achieve using purely dielectric materials can be effectively compensated by the dispersion characteristics of μ_r. Although magnetic loss generally diminishes at high frequencies, it remains crucial for enhancing microwave absorption intensity and broadening the EAB. The relatively low permeability exhibited at elevated frequencies can be attributed to the Snoek limit—a fundamental constraint that governs the relationship between permeability and frequency under natural resonance conditions. The product of static permeability and natural resonance frequency is a constant that is proportional to saturation magnetization. Therefore, to operate effectively at higher frequencies, a compromise involving reduced permeability must be accepted.

To illustrate the role of moderate magnetic loss in designing high-attenuation MAMs for the 8–18 GHz band, a 1 mm-thick reference model (ME1, μ_r'= 1 and μ_r''= 0) was established. Reflecting the practical permeability ranges of natural materials, three additional dielectric–magnetic models (ME2, ME3, ME4) were constructed with μ_r'= 2 and μ_r'' values of 0.2, 0.4, and 0.6, respectively. A computational numerical strategy was employed to optimize the permittivity genome. As depicted in Figs. 2b and 2d, the ideal ε_r-f distributions for ME1–ME4 were derived using the FNN model. Increasing μ_r'' resulted in a clear reduction in both $\Delta\varepsilon_r'$ and $\Delta\varepsilon_r''$. For instance, compared to the purely dielectric system ME1, the value of $\Delta\varepsilon_r'$ for ME4 decreased from 82.6 to 45.3 within the 8–18 GHz range. This moderated dispersion facilitates the practical realization of MAMs with target electromagnetic parameters, thereby enabling ultrathin and broadband

absorption. Although the electromagnetic constants and loss factors are decisive in determining absorption frequency and efficiency, further tuning in complex composite systems remains challenging[26,27,37]. Conventional methods often require iterative performance recalculations based on empirical formulas to align material parameters with optimal dispersion regions. To reduce design complexity, a fundamental reassessment of the relationship between intrinsic EM properties and macroscopic MA performance is essential.

In accordance with Poynting's theorem (**S = E × H**), the flow of electromagnetic energy is governed by the interplay between electric and magnetic fields[15]. The interactions of these fields with various media are characterized by permittivity and permeability, which together determine the electromagnetic response of materials. Furthermore, within the framework of interference cancellation theory, the wavelength of electromagnetic waves in a medium can be expressed as $\lambda_m = c/(f|\mu_r\varepsilon_r|^{1/2})$, illustrating a direct correlation with operating frequency. Finally, results from machine learning optimization indicate a complementary relationship between the variation trends of permeability and permittivity.

Rather than treating permittivity and permeability in isolation, we propose an optimized EFDC ($EFDC = |\mu_r\varepsilon_r| = [(\varepsilon_r')^2 + (\varepsilon_r'')^2]^{1/2}[(\mu_r')^2 + (\mu_r'')^2]^{1/2}$) as a unified parameter to evaluate MA performance under the condition of RL $<$ −10 dB. In contrast to traditional methods, EFDC exhibits a more direct and robust correlation with the intrinsic parameters of the medium. More significantly, it is capable of accurately delineating the requirements for electromagnetic frequency dispersion of materials within the frequency domain. The optimal EFDC-f distributions for ME1–ME4, derived from the FNN model based on transmission line theory (see Supplementary Note 1),

reveal a high degree of consistency across all four models (Figs. 2b–d), despite their divergent ε_r-f profiles. When the optimized parameters are applied in the transmission line model (Supplementary Equation (1–2)), each model achieves over 99% absorption (Fig. 2e), confirming a robust correlation between EFDC and MA performance. This dual-dispersion fusion strategy provides an efficient pathway to approach theoretical performance limits in practical MAM designs, while addressing key challenges in accelerating the development of high-performance microwave absorbers.

Development of ultrathin and broad-band microwave absorbing materials using the electromagnetic frequency dispersion coefficient model

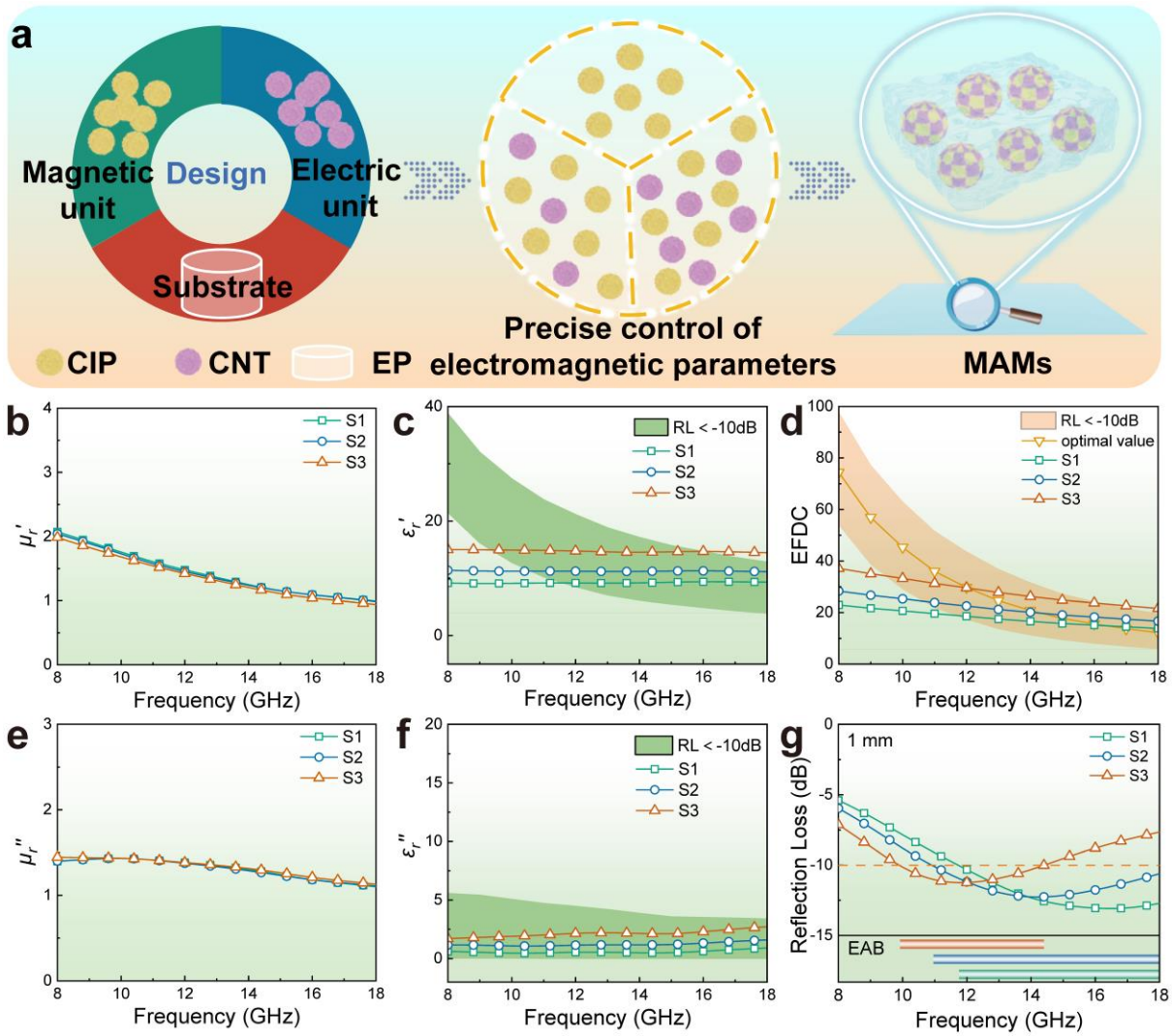

Fig. 3 | Schematic of accurate regulation of electromagnetic parameters and room-temperature electromagnetic characteristics. a Schematic diagram illustrating the fabrication process of the CIP/CNTs/EP composite. **b, e** Real and imaginary parts of complex permeability (μ_r' and μ_r''), **c, f** real and imaginary parts of complex permittivity (ε_r' and ε_r''), **d** electromagnetic frequency dispersion coefficient, and **g** microwave absorption performance for samples S1, S2, and S3 at a thickness of 1 mm. The shaded region indicates the optimized range of electromagnetic parameters corresponding to effective microwave absorption performance (RL $<$ −10 dB).

Based on the preceding analysis, the electromagnetic fusion strategy can be quantitatively characterized through EFDC-f dispersion. The synergistic model correlating EFDC with MA performance provides a targeted design framework for developing high-performance MAMs. Given the excellent electromagnetic loss capabilities of CIP and CNTs, CIP/CNTs/epoxy (EP) composites were fabricated to elucidate the synergistic enhancement arising from combined magnetic and dielectric losses. This study aims to identify the optimal range of electromagnetic parameters that maximize absorption efficiency. To this end, composites with a fixed CIP content of 80 wt.% were selected as a model system to investigate the influence of permittivity on absorption intensity and absorption frequency. Three samples, designated as S1, S2, and S3, were prepared with CNT contents of 0 wt.%, 0.15 wt.%, and 0.2 wt.%, respectively. The compositional characteristics, microstructure, and electromagnetic properties (2–18 GHz) of the samples are provided in Supplementary Figs. 2–4. The effects of varying material parameters were systematically evaluated, as summarized in Fig. 3a.

As shown in Figs. 3b and e, the real and imaginary parts of complex permeability (μ_r' and μ_r'') exhibit consistent dispersion trends across all three composites, which can be attributed to their identical CIP content. This simplifies the tuning of permittivity and facilitates the attainment of optimized electromagnetic parameters over a broad frequency range. Figs. 3c and f demonstrate that increasing the CNT content from 0 wt.% to 0.2 wt.% allows precise modulation of the complex permittivity (ε_r' and ε_r''). For the design of ultrathin and broadband MAM targeting a thickness of 1 mm, electromagnetic parameters were optimized using an EFDC-guided approach. As the relative permittivity is systematically raised, a wider frequency range falls within the optimized

EFDC domain. When the ε_r-f relationship closely matches the simulated optimal dispersion profile, the effective absorption bandwidth (EAB) broadens, while the maximum attenuation peak shifts toward lower frequencies (Figs. 3d and g). These graded electromagnetic properties collectively enhance the attenuation capability of the MAMs while simultaneously modulating their impedance matching characteristics.

The performance of MAMs depends not only on attenuation efficiency but also critically on impedance matching. Excessively high ε_r can cause impedance mismatches, particularly at higher frequencies. The trade-off between attenuation capacity and impedance matching can be quantitatively evaluated using the attenuation constant (α) and impedance matching coefficient (M_z)[38]:

$$\alpha = \frac{\sqrt{2}}{c}\pi f\sqrt{(\varepsilon_r''\mu_r'' - \varepsilon_r'\mu_r') + \sqrt{(\varepsilon_r''\mu_r'' - \varepsilon_r'\mu_r')^2 + (\varepsilon_r''\mu_r' + \varepsilon_r'\mu_r'')^2}} \quad \textbf{(1)}$$

$$M_z = \frac{2Z_{in}'/Z_0}{|Z_{in}/Z_0|^2+1} \quad \textbf{(2)}$$

Z_{in}' represents the real part of Z_{in}. M_z > 0.82 corresponds to a wider EAB. Increasing EFDC leads to higher attenuation constants from S1 to S3, accompanied by a shift of the optimized M_z region toward lower frequencies (Supplementary Fig. 5).

This indicates that EFDC effectively integrates contributions from both permittivity and permeability, thereby improving the control over electromagnetic properties during material preparation. In contrast to purely dielectric composites, this dual-loss mechanism reduces overreliance on a single loss type and more readily satisfies the optimized dispersion requirements over a wide band. Consequently, the microwave absorption performance of broadband MAMs can be effectively tailored using EFDC-based design principles.

As illustrated in Figs. 3d and g, the EFDC of sample S2 closely matches the simulated optimum, yielding a broad EAB of 7.04 GHz at a minimal thickness of 1 mm. Moreover, an EAB of 9.28 GHz has been achieved at a thickness of 1.3 mm, which not only signifies a balanced optimization of both key parameters but also surpasses most current state-of-the-art materials. When compared to previously reported composites such as Fe_3O_4/MWCNTs[39], RGO/Si_3N_4[40], ZnO@MWCNT[41], and Co[42], sample S2 demonstrates the highest specific EAB efficiency (SEAB = 7.04 GHz mm^{-1}) and ranks among the top-performing absorbers, as detailed in Supplementary Table 1. These results confirm that an optimized EFDC-f relationship positions magnetic-dielectric hybrid systems as highly promising candidates for next-generation lightweight and high-performance microwave absorbers.

Development of stable microwave absorbing materials with a wide temperature range using the electromagnetic frequency dispersion coefficient model

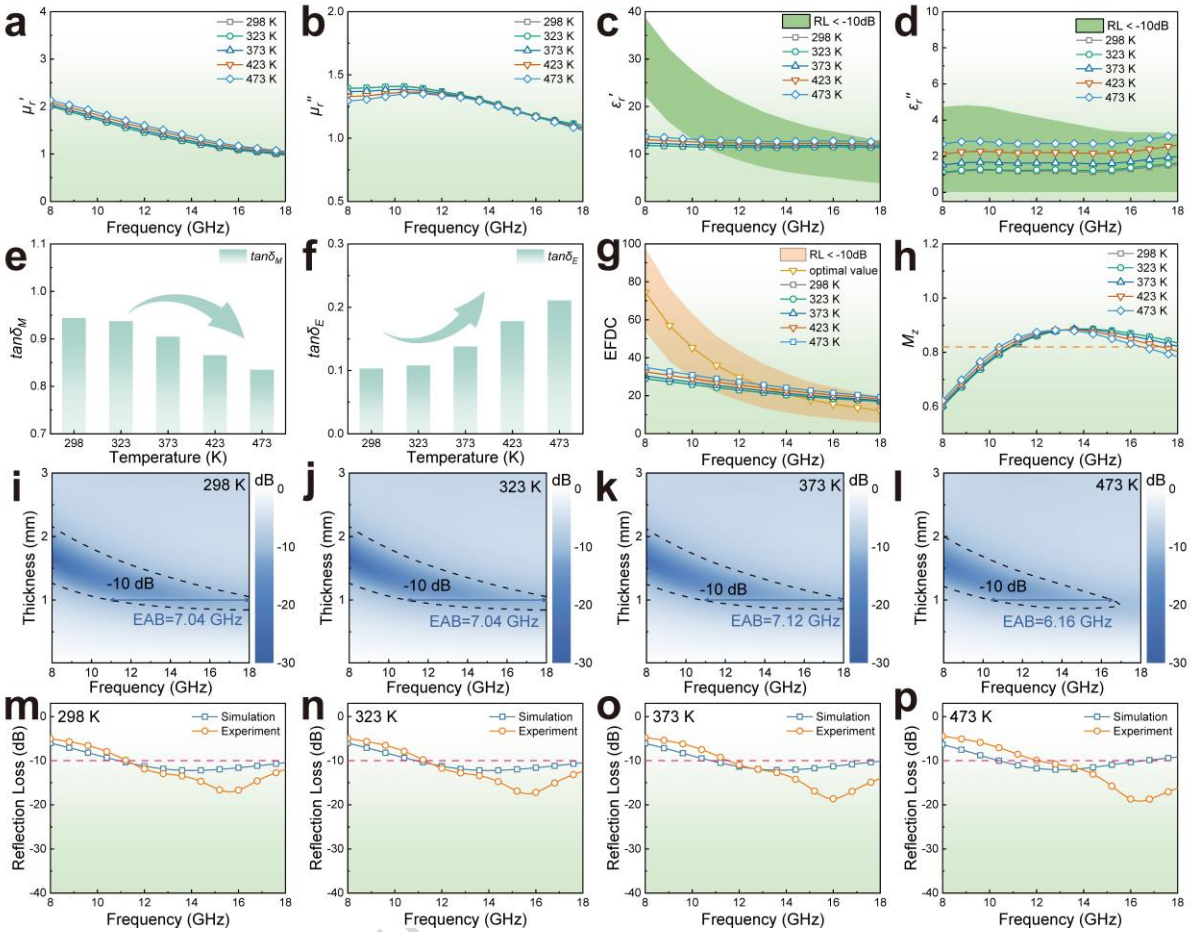

Fig. 4 | Electromagnetic performance over a wide temperature range. a, **b** Real and imaginary parts of complex permeability (μ_r' and μ_r''), **c**, **d** real and imaginary parts of complex permittivity (ε_r' and ε_r''), **e**, **f** magnetic and dielectric loss tangents ($tan\delta_M$ and $tan\delta_E$) of sample S2 at 12 GHz; **g** electromagnetic frequency dispersion coefficient (EFDC) and **h** normalized impedance matching degree (M_z); **i-p** microwave absorption performance under varying temperatures.

When deploying MAMs in high-temperature applications, it is critical that they not only exhibit high thermal resistance but also maintain performance stability across a broad temperature spectrum. Generally, as temperature increases, dielectric loss is governed by both conductive loss

(ε_c'') and polarization loss (ε_p'')[43]. Both components are functions of temperature and frequency: $\varepsilon_r'' = \varepsilon_p'' + \varepsilon_c'' = (\varepsilon_s - \varepsilon_\infty)\frac{\omega\tau}{1+\omega^2\tau(T)^2} + \frac{\sigma(T)}{\varepsilon_0\omega}$, where ω is angular frequency and τ is relaxation time, $\sigma(T)$ is temperature-dependent conductivity, ε_∞, ε_0, and ε_s represent the relative permittivity (ε_r) at infinite frequency, in vacuum and under static conditions, respectively[44].

Although rising temperature typically enhances conductive loss—leading to greater EMWs attenuation—the overall absorption performance often deteriorates due to degraded impedance matching[45]. As a result, MAMs tend to exhibit increased reflection behavior at elevated temperatures. Most current strategies seek to modulate conductivity and polarization to improve impedance matching under thermal variation; however, these approaches often come at the cost of reduced loss capability. Thus, an ideal MAM should simultaneously achieve good impedance matching and strong loss performance across a wide temperature range.

In contrast to the generally increasing trend of ε_r with increasing temperature, the saturation magnetization of magnetic components typically declines due to the Curie temperature limit[46]. Concurrently, enhanced damping of magnetic moment precession reduces natural resonance at elevated temperatures, resulting in a decrease in μ_r'' [47]. The opposing thermal responses of permittivity and permeability make it challenging to achieve stable MA over a broad temperature span. Therefore, leveraging the complementary dispersion behavior of magnetic-dielectric systems offers a promising design pathway. Although magnetic loss may be relatively weak at high frequencies and temperatures, it still contributes critically to enhancing absorption intensity and widening the EAB. This approach helps stabilize the EFDC under thermal changes. A consistent EFDC promotes temperature-insensitive MA performance by sustaining stable EMW–matter

interactions and facilitating interference cancellation. Thus, properly accounting for the role of magnetic loss—even when modest—enables the design of ultrathin, broadband MAMs with reliable high-temperature performance.

As the temperature increases from 298 K to 473 K, the real part of permeability (μ_r') in sample S2 remains largely stable, while the imaginary part (μ_r'') slightly decreases, leading to a reduction in $tan\delta_M$ (Figs. 4a, b and e). In contrast, the high conductivity of CNTs causes both ε_r' and ε_r'' to rise, accompanied by an increase in $tan\delta_E$ (Figs. 4c, d and f). Simulation results further confirm that the optimal permittivity distribution remains within an acceptable range at elevated temperatures.

A crucial compensation mechanism is identified: the decline in magnetic loss from CIP is effectively offset by a concurrent rise in dielectric loss from CNTs. This dynamic balance maintains optimal attenuation (Supplementary Fig. 6) while preventing impedance mismatch caused by excessive losses. Furthermore, the stable EFDC across temperatures suggests a nearly constant microwave wavelength in the material, ensuring consistent interference cancellation. Thanks to the complementary thermal responses of μ_r and ε_r, both EFDC and M_z show minimal temperature dependence (Figs. 4g and h), leading to stable microwave absorption that converges toward the optimum in the 11–18 GHz band (Figs. 4i–l). For instance, sample S2 retains an EAB above 7.04 GHz from 298 K (Fig. 4i) to 373 K (Fig. 4k). Even at 473 K (Fig. 4l), it still achieves an EAB exceeding 6.16 GHz, demonstrating satisfied thermal stability.

To assess practical applicability, a square sheet (180 mm × 180 mm × 1 mm) of the CIP/CNTs/EP composite (sample S2) was fabricated. Its MA performance was evaluated using an in-situ arc

method (Supplementary Fig. 7), with reflection loss (RL) calculated as: $RL(\mathrm{dB}) = 10lg(P_r/P_i)$, where P_r and P_i represent the power of reflected and incident waves, respectively[48]. Remarkably, this ultrathin (1 mm) composite achieves an EAB of up to 6.8 GHz. As evidenced by the excellent agreement between simulation and experiment (Figs. 4m–p and Supplementary Fig. 8), the designed broadband absorber successfully maintains stable microwave absorption across a wide temperature range.

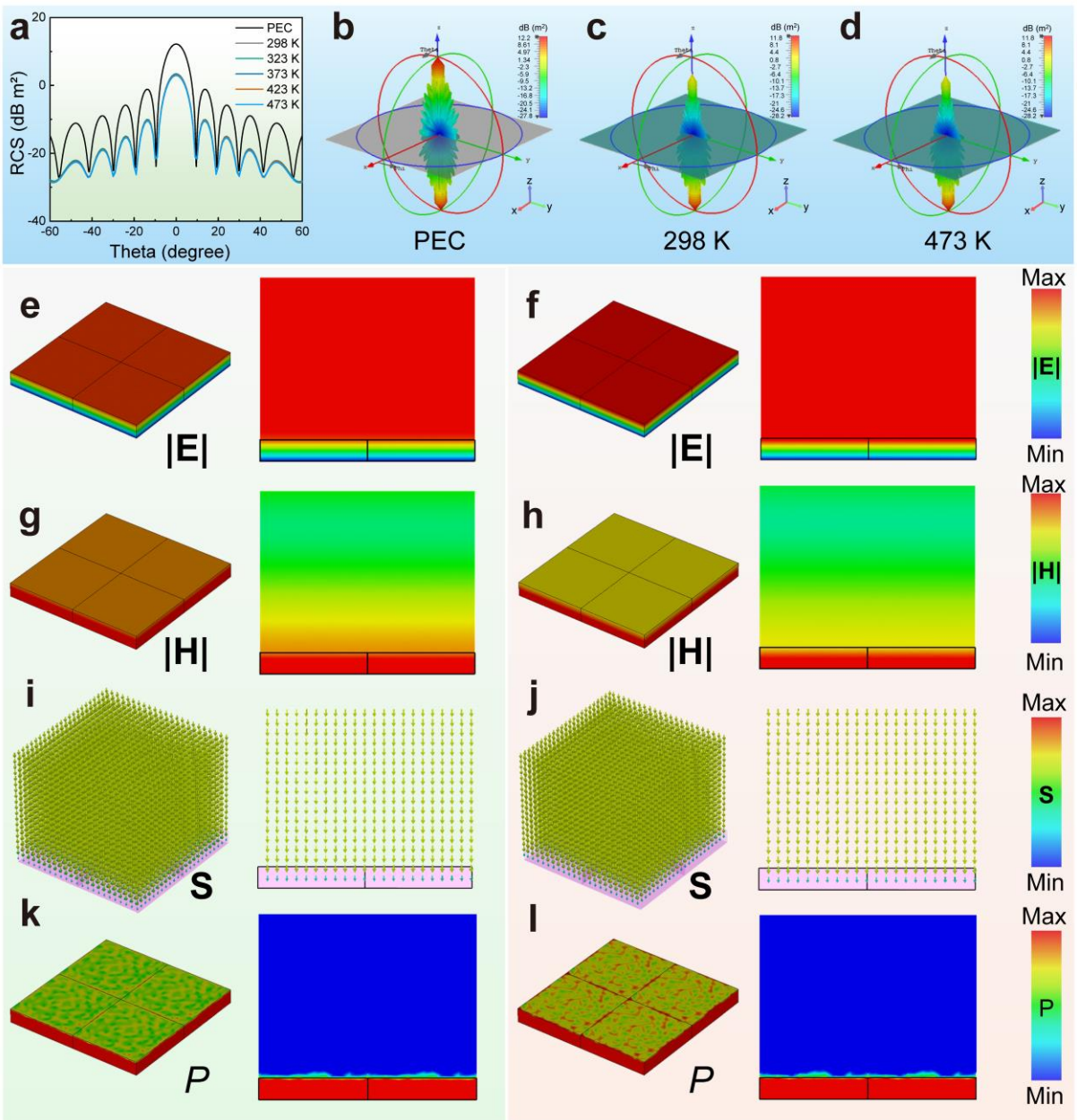

Fig. 5 | Simulated electromagnetic field distribution. a Radar cross-section (RCS) of sample S2 as a function of detection angle ($-60° < \theta < 60°$) under various temperatures. Far-field scattering patterns of **b** perfect electric conductor (PEC), and sample S2 at **c** 298 K and **d** 473 K. Simulated distributions of **e, f** electric field intensity (|**E**|), **g, h** magnetic field intensity (|**H**|), **i, j** Poynting vector (**S**), and **k, l** power loss density (*P*) for S2 at 298 K and 473 K.

To further evaluate the stealth performance under far-field conditions, the radar cross-section (RCS) of sample S2 was simulated using CST Microwave Studio at 10 GHz, as shown in Figs. 5a–d. In contrast to the perfect electric conductor (PEC) plate (Fig. 5b), sample S2 exhibits substantial electromagnetic wave (EMW) attenuation across a temperature range of 298 K to 473 K, demonstrating stable and robust microwave absorption (MA) characteristics (Figs. 5c–d). The electric and magnetic field distributions of sample S2 were analyzed at 298 K and 473 K (Figs. 5e–l). It is observed that the electric field magnitude |**E**| within the CIP/CNTs/EP composite increases with temperature, while the magnetic field magnitude |**H**| decreases. This suggests an enhanced electric response during EMWs–material interactions (Figs. 5e–f), accompanied by a reduced magnetic component (Figs. 5g–h). Notably, both the Poynting vector (**S**) (Figs. 5i–j) and power loss density (*P*) (Figs. 5k–l) remain largely unaffected by temperature, indicating excellent thermal stability in energy dissipation. These results are consistent with our previous conclusion that a well-designed magnetic-dielectric composite can maintain consistent MA performance despite variations in individual electromagnetic parameters. Furthermore, this study demonstrates that EFDC, derived through inverse design via FNN modeling, provides an effective strategy for developing high-performance MAMs.

This approach mitigates the extensive resource and time investments typical of high-throughput experimentation while delivering performance that surpasses conventional limits. The proposed methodology thus establishes an efficient and versatile pathway for designing customizable microwave absorbers with superior thermal adaptability.

Development of ultra-strong microwave absorption performance using the electromagnetic frequency dispersion coefficient model

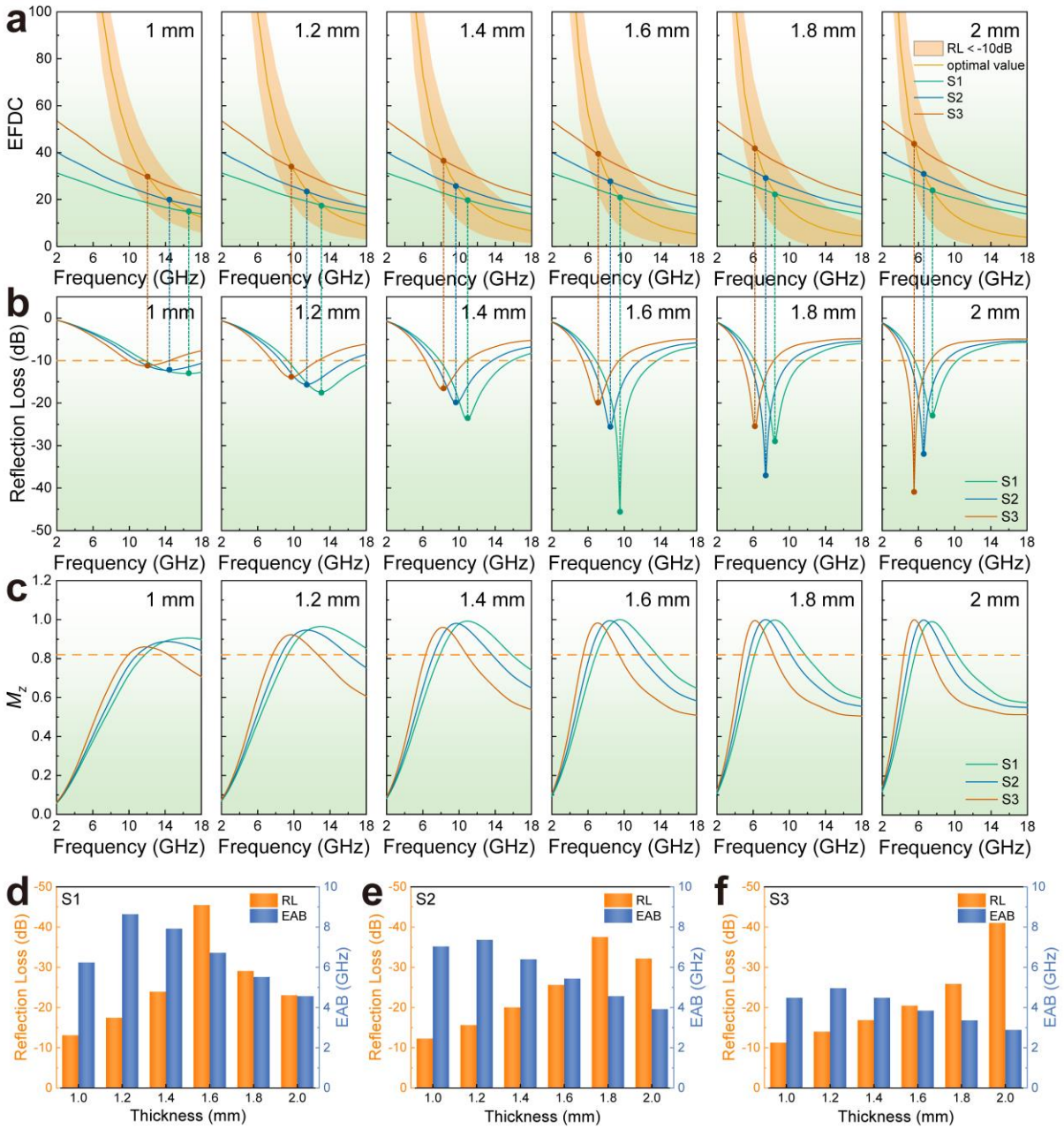

Fig. 6 | Guidance from EFDC for strong microwave absorption. a Electromagnetic frequency dispersion coefficient (EFDC), **b** microwave absorption (MA) performance and **c** normalized impedance matching degree (M_z) of samples S1, S2, and S3 at thicknesses of 1 mm, 1.2 mm, 1.4

mm, 1.6 mm, 1.8 mm and 2 mm. **d**–**f** Minimum reflection loss (RL_{min}) and effective absorption bandwidth (EAB) of S1, S2, and S3 as functions of thickness.

In addition to excellent ultrathin and broadband microwave absorption (MA) performance, achieving ultra-strong absorption is essential for developing high-efficiency MAMs[49]. As established in the preceding analysis, the simulated optimal EFDC provides precise guidance for enhancing ultra-strong MA performance (orange curves in Fig. 6a), calculated here for thicknesses of 1 mm, 1.2 mm, 1.4 mm, 1.6 mm, 1.8 mm and 2 mm. The EFDC curves of samples S1, S2, and S3 exhibit multiple intersection points that align with the optimal MA positions defined by their electromagnetic parameters (Supplementary Fig. 4), further corroborated in Fig. 6b. Moreover, the optimal absorption frequency (Fig. 6b) and optimal M_z (Fig. 6c) shift toward lower frequencies, a trend attributed to progressive increases in both the attenuation constant (Supplementary Fig. 9) and EFDC values. This behavior underscores a clear correlation between reduced thickness and elevated EFDC. As illustrated in Fig. 6b, sample S1 achieves an exceptional absorption intensity of -45.45 dB at a thickness of only 1.6 mm. Furthermore, as shown in Supplementary Fig. 10, each sample attains remarkable MA intensities of −50.84 dB, −53.36 dB, and −51.19 dB through fine-tuned EFDC modulation. A comprehensive overview of MA intensity and effective absorption bandwidth (EAB) across different thicknesses is presented in Figs. 6d–f, highlighting excellent absorption performance. The proposed magnetic-dielectric dual-dispersion strategy successfully identifies electromagnetic parameters that meet the demanding requirements of advanced MAMs.

This approach enables the tailored design of absorbers featuring ultrathin profiles, wide bandwidth, and exceptional absorption strength (Supplementary Fig. 11).

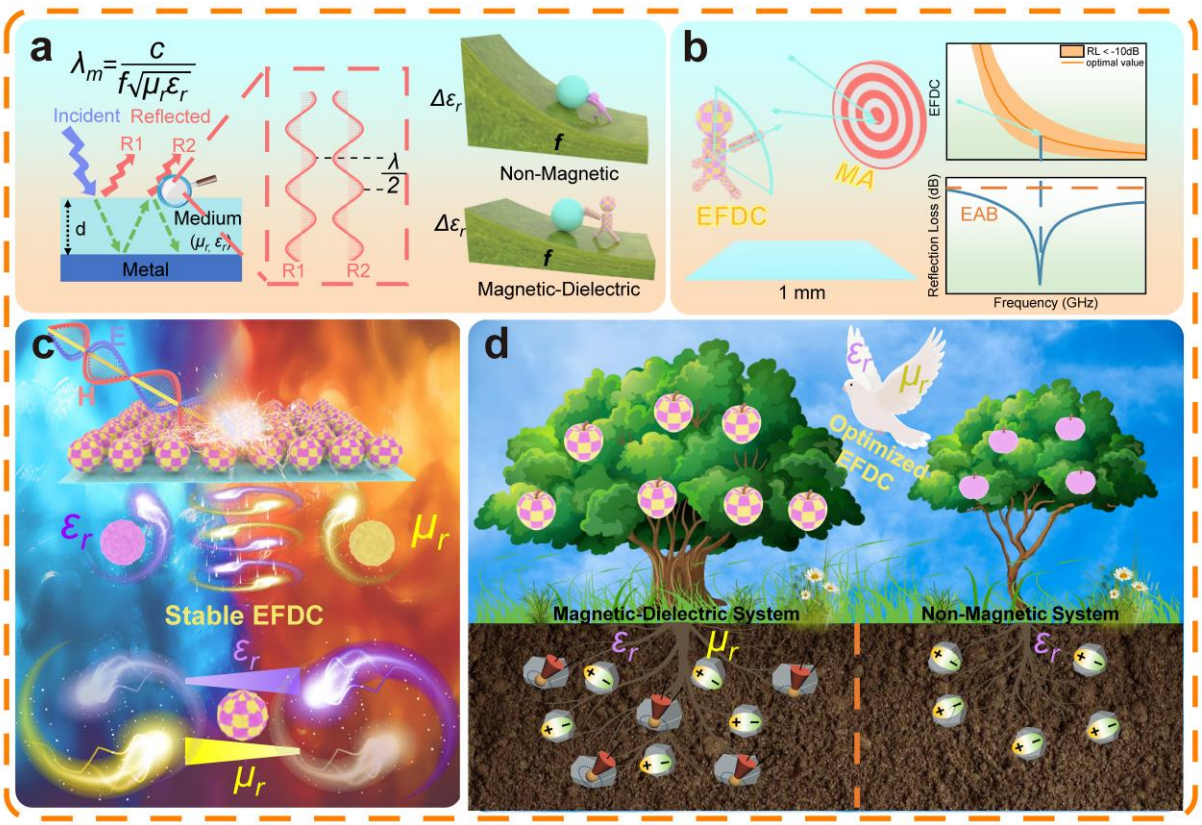

Fig. 7 | Schematic illustration of the microwave dissipation mechanism in the optimized magnetic-dielectric system. a Enhanced magnetic loss relaxes the stringent frequency dispersion requirement for ε_r. **b, d** Design strategy for ultrathin broadband microwave absorbing materials guided by the electromagnetic frequency dispersion coefficient (EFDC) principle. **c** Synergistic effects between magnetic and dielectric losses under varying temperature conditions.

Based on the preceding analysis, magnetic loss proves to be an indispensable factor, as it effectively relaxes the stringent dispersion constraints on the ε_r-f relationship while further improving MA performance (Fig. 7). Through precise regulation of EM parameters, the

interference cancellation of electromagnetic waves can be effectively manipulated, leading to enhanced MA efficiency (Fig. 7a). Furthermore, the EFDC comprehensively incorporates contributions from both ε_r and μ_r, thereby circumventing associated with individual EM parameters. This strategy offers critical insights for the tailored design of MAMs, ultimately achieving an ultra-wide bandwidth of 7.04 GHz at a small thickness of 1.0 mm (Fig. 7b). Moreover, an optimal balance between magnetic and electric components has been realized, which promotes efficient impedance matching while maintaining a stable dynamic equilibrium of ε_r and μ_r across a wide temperature range. This synergy facilitates deeper penetration of electromagnetic waves into the absorber, where they are subsequently attenuated through combined magnetic and dielectric loss mechanisms, resulting in a strong absorption intensity of −53.36 dB (Fig. 7c).

In contrast to non-magnetic composites (Fig. 7d), materials incorporating magnetic components significantly broaden the acceptable range of ε_r - f dispersion, enabling performance that approaches theoretical limits. This is demonstrated through an optimal integration of minimal thickness, broad bandwidth, excellent thermal stability, and strong absorption. A detailed comparison of the MA performance with previously reported absorbers is provided in Supplementary Table 1. Thus, the EFDC-guided approach not only identifies optimal EM parameter windows but also achieves target-specific MA performance under given constraints, offering a valuable design paradigm for developing advanced broadband microwave absorbers.

Discussion

In conclusion, this study proposes an EFDC-based strategy that constructs a quantitative relationship between intrinsic electromagnetic parameters and macroscopic MA performance. The

FNN model validates the role of EFDC as a pivotal design metric, enabling optimized coordination between complex permittivity and permeability. By enhancing magnetic loss, this method alleviates the stringent frequency dispersion requirements traditionally imposed on ε_r, thus streamlining the parameter design process for broadband MAMs. Moreover, the stability of EFDC ensures effective MA performance over a wide temperature range (298–473 K), even as the electric and magnetic properties exhibit divergent trends under thermal variation. The proposed methodology adopts an efficient two-step calibration process: initial coarse adjustment of electromagnetic components followed by EFDC-guided fine-tuning, which collectively enhances wave absorption through optimized interference cancellation. This approach enables the development of an ultrathin absorber (1 mm) with an ultra-wide bandwidth of 7.04 GHz, a remarkable absorption intensity of −53.36 dB, and excellent thermal stability. Overall, this work establishes a comprehensive and systematic framework for designing high-performance MAMs with customizable absorption properties, offering valuable insights into the targeted development of advanced electromagnetic functional materials for complex operational environments.

Methods

Materials

To achieve tailored electromagnetic properties—specifically, tunable complex permeability (μ_r) and permittivity (ε_r)—along with precise regulation of EFDC, magnetic-dielectric composites were fabricated using carbon nanotubes (CNTs, Qianying New Materials Technology Co., LTD) as the dielectric loss component and carbonyl iron powder (CIP, Jiangsu Shisong New Materials

Technology Co., LTD) as the magnetic loss component. Epoxy resin (EP, Nantong Xingchen Synthetic Materials Co., LTD was chosen as the matrix material owing to its stable permittivity.

Preparation of CIP/CNTs/EP composites

CIP/EP composites are prepared by incorporating 80 wt.% CIP into the EP matrix along with a curing agent, followed by mixing at 2000 r min^{-1} for 5 minutes. The homogeneous mixture was then poured into a mold and cured at 80 °C for 8 hours, yielding sample S1. Using the same procedure, CNTs were introduced into the CIP/EP composite at mass fractions of 0.15 wt.% and 0.2 wt.%, producing samples S2 and S3, respectively. The final samples were processed into coaxial rings with an inner diameter of 3.04 mm, an outer diameter of 7 mm, and a thickness of 2 mm.

Characterization

The composition of CIP and CNTs was characterized by X-ray diffractometry (XRD, D8-Advance, Bruker) and Raman spectroscopy (Raman, RM-1000, 532 nm, Renishaw), respectively. Morphological analysis was performed using scanning electron microscopy (SEM, Carl Zeiss Gemini 500). The electromagnetic parameters of the CIP/CNTs/EP composites were measured from 298 K to 473 K using a vector network analyzer (VNA, 3672B-S, Ceyear). Finally, sample S2 was processed into a film with dimensions of 180 mm × 180 mm × 1 mm, and its microwave absorption performance was evaluated over the same temperature range using an arch reflection test system. The temperature was ramped at a constant rate of 10 K min^{-1} throughout the tests. At each target temperature (298, 323, 373, 423, and 473 K), a 10-minute isothermal hold was applied, and measurements were taken upon stabilization after this period.

Electromagnetic simulations

Electromagnetic simulations are described in Supplementary Notes 1 to 4.

Data availability

The data that support the findings of this study are provided in the main text and the Supplementary Information. Source data are provided with this paper.

References

1 Tao, J. *et al.* Phenolic multiple kinetics-dynamics and discrete crystallization thermodynamics in amorphous carbon nanostructures for electromagnetic wave absorption. *Nat. Commun.* **15**, 10337 (2024).

2 Liu, X. *et al.* Modulating Electromagnetic Genes Through Bi-Phase High-Entropy Engineering Toward Temperature-Stable Ultra-Broadband Megahertz Electromagnetic Wave Absorption. *Nano-Micro Lett.* **17**, 164 (2025).

3 Liu, A. *et al.* Asymmetric Structural MXene/PBO Aerogels for High-Performance Electromagnetic Interference Shielding with Ultra-Low Reflection. *Adv. Mater.* **37**, 2414085 (2025).

4 Sun, Z. *et al.* Anti-radar based on metasurface. *Nat. Commun.* **16**, 7258 (2025).

5 Tao, J. *et al.* Anionic high-entropy doping engineering for electromagnetic wave absorption. *Nat. Commun.* **16**, 3163 (2025).

6 Shu, J. C., Zhang, Y. L., Qin, Y. & Cao, M. S. Oxidative Molecular Layer Deposition Tailoring Eco-Mimetic Nanoarchitecture to Manipulate Electromagnetic Attenuation and Self-Powered Energy Conversion. *Nano-Micro Lett.* **15**, 142 (2023).

7 Zhang, Y. *et al.* Broadband and tunable high-performance microwave absorption of an ultralight and highly compressible graphene foam. *Adv. Mater.* **27**, 2049-2053 (2015).

8 Qu, N. *et al.* 2D/2D coupled MOF/Fe composite metamaterials enable robust ultra-broadband microwave absorption. *Nat. Commun.* **15**, 5642 (2024).

9 Wang, Z. Y. *et al.* Functional Carbon Springs Enabled Dynamic Tunable Microwave Absorption and Thermal Insulation. *Adv. Mater.* **36**, 2412605 (2024).

10 Lv, H. L. *et al.* Insights into Civilian Electromagnetic Absorption Materials: Challenges and Innovative Solutions. *Adv. Funct. Mater.*, 2315722 (2024).

11 Cheng, J. Y. *et al.* Emerging Materials and Designs for Low- and Multi-Band Electromagnetic Wave Absorbers: The Search for Dielectric and Magnetic Synergy? *Adv. Funct. Mater.* **32**, 2200123 (2022).

12 Zhao, Z. *et al.* Advancements in Microwave Absorption Motivated by Interdisciplinary Research. *Adv. Mater.* **36**, 2304182 (2024).

13 Hao, B. *et al.* Multiscale Design of Dielectric Composites for Enhanced Microwave Absorption Performance at Elevated Temperatures. *Adv. Funct. Mater.*, 2423897 (2025).

14 Liu, X. *et al.* $FeCoNiCr_{0.4}Cu_X$ High-Entropy Alloys with Strong Intergranular Magnetic Coupling for Stable Megahertz Electromagnetic Absorption in a Wide Temperature Spectrum. *ACS Appl. Mater. Interfaces* **14**, 7012-7021 (2022).

15 Yang, J. M. *et al.* Construction of in-situ grid conductor skeleton and magnet core in biodegradable poly (butyleneadipate-co-terephthalate) for efficient electromagnetic interference shielding and low reflection. *Compos. Sci. Technol.* **240**, 110093 (2023).

16 Zhou, L. *et al.* Harnessing the Electronic Spin States of Single Atoms for Precise Electromagnetic Modulation. *Adv. Mater.* **37**, 2418321 (2025).

17 Cai, B. *et al.* Interface-induced dual-pinning mechanism enhances low-frequency electromagnetic wave loss. *Nat. Commun.* **15**, 3299 (2024).

18 Wu, Z. *et al.* Dimensional Design and Core-Shell Engineering of Nanomaterials for Electromagnetic Wave Absorption. *Adv. Mater.* **34**, 2107538 (2022).

19 Guo, Y. *et al.* Carbon Nanocoils-Assisted Formation of Tunable Pore Graphene Aerogels for Lightweight Broadband Microwave Absorption, Thermal Insulation, and Antifreeze Devices. *Small* **21**, 2412270 (2025).

20 Zhao, R. Z. *et al.* Highly anisotropic Fe3C microflakes constructed by solid-state phase transformation for efficient microwave absorption. *Nat. Commun.* **15**, 1497 (2024).

21 Rozanov, K. N. Ultimate Thickness to Bandwidth Ratio of Radar Absorbers. *IEEE Trans. Antennas Propag.* **48**, 1230 (2000).

22 Ren, B. *et al.* Achieving broadband electromagnetic absorption at a wide temperature range up to 1273 K by metamaterial design on polymer-derived SiC-BN@CNT ceramic composites. *Chem. Eng. J.* **478**, 147251 (2023).

23 Gai, L. *et al.* Compositional and Hollow Engineering of Silicon Carbide/Carbon Microspheres as High-Performance Microwave Absorbing Materials with Good Environmental Tolerance. *Nano-Micro Lett.* **16**, 167 (2024).

24 Zhong, X. *et al.* Heterostructured BN@Co-C@C Endowing Polyester Composites Excellent Thermal Conductivity and Microwave Absorption at C Band. *Adv. Funct. Mater.* **23**, 13544 (2024).

25 He, M. *et al.* Excellent Low-Frequency Microwave Absorption and High Thermal Conductivity in Polydimethylsiloxane Composites Endowed by Hydrangea-Like CoNi@BN Heterostructure Fillers. *Adv. Mater.* **36**, 2410186 (2024).

26 Fang, G. *et al.* The Elaborate Design of Multi-Polarization Effect by Non-Edge Defect Strategy for Ultra-Broad Microwave Absorption. *Adv. Funct. Mater.* **34** (2024).

27 Zeng, X., Nie, T., Zhao, C., Gao, Y. & Liu, X. In Situ Exsolution-Prepared Solid-Solution-Type Sulfides with Intracrystal Polarization for Efficient and Selective Absorption of Low-Frequency Electromagnetic Wave. *Adv. Sci.* **11**, 2403723 (2024).

28 Zhao, T. B., Lan, D., Jia, Z. R., Gao, Z. G. & Wu, G. L. Hierarchical porous molybdenum carbide synergic morphological engineering towards broad multi-band tunable microwave absorption. *Nano Res.* **17**, 9845-9856 (2024).

29 Zhang, Q. L. *et al.* Constructing multiple heterogeneous interfaces in one-dimensional carbon fiber materials for superior electromagnetic wave absorption. *Carbon* **226**, 119233 (2024).

30 Gao, Y. *et al.* Multifunction integration within magnetic CNT-bridged MXene/CoNi based phase change materials. *eScience* **4**, 100292 (2024).

31 Zhang, K. L. *et al.* Tracking Regulatory Mechanism of Trace Fe on Graphene Electromagnetic Wave Absorption. *Nano-Micro Lett.* **16**, 66 (2024).

32 Yan, Y. F. *et al.* Phase Engineering on MoS_2 to Realize Dielectric Gene Engineering for Enhancing Microwave Absorbing Performance. *Adv. Funct. Mater.* **34**, 2316338 (2024).

33 Shi, Y. Y. *et al.* Well-matched impedance of polypyrrole-loaded cotton non-woven fabric/polydimethylsiloxane composite for extraordinary microwave absorption. *Compos. Sci. Technol.* **197**, 108246 (2020).

34 Song, W. L. *et al.* A universal permittivity-attenuation evaluation diagram for accelerating design of dielectric-based microwave absorption materials: A case of graphene-based composites. *Carbon* **118**, 86-97 (2017).

35 Li, X. L. *et al.* Self-Assembly Core–Shell Graphene-Bridged Hollow MXenes Spheres 3D Foam with Ultrahigh Specific EM Absorption Performance. *Adv. Funct. Mater.* **28**, 1803938 (2018).

36 Li, J. Z. *et al.* Permittivity genome: A new perspective on absorbing materials design. *Chem. Eng. J.* **503**, 158398 (2025).

37 Liu, S. C. *et al.* Arousing effective attenuation mechanism of reduced graphene oxide-based composites for lightweight and high efficiency microwave absorption. *Appl. Phys. Lett.* **113**, 083905 (2018).

38 Hou, Z. L., Gao, X. S., Zhang, J. Y. & Wang, G. S. A perspective on impedance matching and resonance absorption mechanism for electromagnetic wave absorbing. *Carbon* **222**, 118935 (2024).

39 Lu, M. M. *et al.* Multiscale Assembly of Grape-Like Ferroferric Oxide and Carbon Nanotubes: A Smart Absorber Prototype Varying Temperature to Tune Intensities. *ACS Appl. Mater. Interfaces* **7**, 19408-19415 (2015).

40 Hou, Z. X. *et al.* Reduced Graphene Oxide/Silicon Nitride Composite for Cooperative Electromagnetic Absorption in Wide Temperature Spectrum with Excellent Thermal Stability. *ACS Appl. Mater. Interfaces* **11**, 5364-5372 (2019).

41 Lu, M. M. *et al.* Multi-wall carbon nanotubes decorated with ZnO nanocrystals: mild solution-process synthesis and highly efficient microwave absorption properties at elevated temperature. *J. Mater. Chem. A* **2**, 10540–10547 (2014).

42 Wang, G. W. *et al.* Microwave absorption properties of flake-shaped Co particles composites at elevated temperature (293–673 K) in X band. *J. Magn. Magn. Mater.* **456**, 92-97 (2018).

43 Zhang, Y. H. *et al.* TiN nanofiber metacomposites for efficient electromagnetic wave absorption: Insights on multiple reflections and scattering effects. *J. Mater. Sci. Technol.* **233**, 69-79 (2025).

44 Li, C. *et al.* Interface Engineering of Titanium Nitride Nanotube Composites for Excellent Microwave Absorption at Elevated Temperature. *Nano-Micro Lett.* **16**, 168 (2024).

45 Zhao, Y. M. *et al.* Simple synthesis of hollow CoFe carbon fiber composites with enhanced heterogeneous interfaces and impedance matching for broadband microwave absorption. *J. Mater. Sci. Technol.* **238**, 178-190 (2025).

46 Li, Z. R. *et al.* Strategy-Induced Strong Exchange Interaction for Enhancing High-Temperature Magnetic Loss in High-Entropy Alloy Powders. *Adv. Funct. Mater.* (2025).

47 Yu, M. *et al.* Yolk–shell Fe_3O_4@ZrO_2 prepared by a tunable polymer surfactant assisted sol–gel method for high temperature stable microwave absorption. *J. Mater. Chem. C* **2**, 7275-7283 (2014).

48 Yang, X. *et al.* Bio-Inspired Microwave Modulator for High-Temperature Electromagnetic Protection, Infrared Stealth and Operating Temperature Monitoring. *Nano-Micro Lett.* **14**, 28 (2021).

49 Li, H. *et al.* High-frequency FeSiAl-based soft magnetic composites via simultaneously suppressed eddy and hysteresis losses. *Nat. Commun.* **16**, 9563 (2025).

Acknowledgments

This work is financially supported by the National Natural Science Foundation of China (No. 22475065) (C.H.G) and (No. 22305066) (C.P.L).

Author contributions

J.W.Z. and C.H.G. gave the research direction and contributed the basic framework and feasible technical route of the project. H.X.S. and Y.Z. conceived the idea, carried out the theoretical analysis and numerical simulations. H.X.S., Y.Z., M.L. and Z.H.C. built up the system and performed the experimentalmeasurements. H.X.S. and C.P.L. performed the data analysis. J.W.Z. and C.H.G. provided the standard experimental site and equipment. H.X.S., C.P.L. and C.H.G. wrote the manuscript. All authors discussed the theoretical aspects and numerical simulations, interpreted the results, and reviewed the manuscript.

Competing interests

The authors declare no competing interests.

Editorial Summary

The authors introduce the Electromagnetic Frequency Dispersion Coefficient (EFDC), a unified parameter linking material properties to microwave absorption. It enables ultra-thin, broadband absorption with record performance and stable operation across temperatures, simplifying the design of advanced absorbing materials.

Peer review information: *Nature Communications* thanks Junwei Gu and the other, anonymous, reviewer(s) for their contribution to the peer review of this work. A peer review file is available.